Veterinary Microbiology 239 (2019) 108489

Contents lists available at ScienceDirect

Veterinary Microbiology

journal homepage: www.elsevier.com/locate/vetmic

Attenuation and characterization of *porcine enteric alphacoronavirus* strain GDS04 *via* serial cell passage

Zhichao Xu[a,1], Ying Lin[a,1], Chuangchao Zou[a], Peng Peng[a], Yanan Wu[b], Ying Wei[a], Yuan Liu[a], Lang Gong[c], Yongchang Cao[a], Chunyi Xue[a,*]

[a] State Key Laboratory of Biocontrol, School of Life Science, Sun Yat-sen University, Guangzhou, 510006, China
[b] College of Animal Science and Veterinary Medicine, Henan Agricultural University, Zhengzhou, 450046, China
[c] College of Veterinary Medicine, South China Agricultural University, Guangzhou, 510642, China

ARTICLE INFO

Keywords:
Porcine enteric alphacoronavirus
Attenuation
Pathogenicity
Newborn piglets
Genomic analysis

ABSTRACT

Porcine enteric alphacoronavirus (PEAV) is a newly identified swine enteropathogenic coronavirus that causes watery diarrhea in newborn piglets. In this study, an original, highly virulent PEAV strain GDS04 was serially passaged in Vero cells. The virus titers and sizes of syncytia increased gradually with the cell passages. Newborn piglets were orally inoculated with PEAV P15, P67 and P100. Compared with P15 and P67, P100 resulted in only mild clinical signs and intestinal lesions in piglets. The virus shedding in feces and viral antigens in intestinal tract were markedly reduced in P100-inoculated piglets. Importantly, all P100-inoculated newborn piglets survived, indicating that P100 was an attenuated variant. Sequence analysis revealed that the virulent strain GDS04 had four, one, six and eleven amino acid differences in membrane, nucleocapsid, spike and ORF1ab proteins, respectively, from P100. Furthermore, more differences in the predicted three-dimensional structure of S protein between GDS04 and P100 were observed, indicating that these differences might be associated with the pathogenicity of PEAV. Collectively, our research successfully prepared a PEAV attenuated variant which might serve as a live attenuated vaccine candidate against PEAV infection.

1. Introduction

Porcine enteric alphacoronavirus (PEAV) was first detected by our team *via* genomic analysis of samples collected from a diarrhea-outbreak swine herds routinely vaccinated with porcine epidemic diarrhea virus (PEDV) vaccine in a farm in Guangdong, China in February 2017 (Gong et al., 2017). This novel swine enteric coronavirus emerged in China at least since August 2016 and it has been widely detected in Guangdong, China, with a prevalence of 43.53% by a retrospective detection study (Zhou et al., 2019). Recently a PEAV-like strain CN/FJWT/2018 was recently discovered in Fujian, China (Li et al., 2018), indicating a prevailing trend in pig farms.

Since the first report, the complete genome of the PEAV strain GDS04 was sequenced (Gong et al., 2017). PEAV is an enveloped, single-stranded, positive-sense RNA virus with a genome of appropriately 27 kb in length (Gong et al., 2017). The genome organization of PEAV is similar to that of bat-like HKU2 strains of coronavirus, with an order of: 5′ untranslated region (UTR), open reading frame 1a/1b (ORF1a/1b), spike (S), nonstructural protein 3 (NS3), envelope (E), membrane (M), nucleocapsid (N), nonstructural protein 7a (NS7a), and 3′ UTR (Lau et al., 2007). The S protein of coronaviruses (CoVs), the pivotal surface glycoprotein, is involved in virus attachment and entry, and induction of neutralizing antibodies *in vivo* (Cruz et al., 2008; Woo et al., 2010). GDS04 strain of PEAV has the smallest S protein among all CoVs (Gong et al., 2017).

The clinical symptoms caused by PEAV in newborn piglets are similar to that by other porcine enteric pathogens such as PEDV and transmissible gastroenteritis virus (TGEV), which include vomiting, diarrhea, dehydration, and mortality rate as high as 90% (Gong et al., 2017; Zhou et al., 2018b). Since PEAV was detected (Gong et al., 2017), another two swine enteric HKU2-related CoVs named SADS-CoV and SeACoV were identified in the same region, causing same diarrheal disease as PEAV strain GDS04 by experimental infection (Pan et al., 2017; Xu et al., 2019a; Zhou et al., 2018b).

Currently, live-attenuated vaccine has been widely used to prevent and control porcine enteric pathogens, such as PEDV, with good clinical effect (Song et al., 2007). Live-attenuated vaccine is prepared from less virulent strain. The virulence of pathogenic microorganisms was

* Corresponding author at: School of Life Science, Sun Yat-sen University, Higher Education Mega Center, Guangzhou, 510006, China.
E-mail address: xuechy@mail.sysu.edu.cn (C. Xue).
[1] These authors have contributed equally to this work.

https://doi.org/10.1016/j.vetmic.2019.108489
Received 19 June 2019; Received in revised form 14 October 2019; Accepted 27 October 2019
0378-1135/

reduced by various methods (Blanco-Lobo et al., 2019; Jie et al., 2018; O'Donnell et al., 2015), such as genetic manipulation (O'Donnell et al., 2015), and cell passage is the most commonly used (Jie et al., 2018). Usually, the virulent parent strain was continuously inoculated cell lines more than 100 generations *in vitro*, and in this process, some mutations will happen in the viral genome, which might lead to the strain's virulence reduce. These cell-passaged strains are then tested in animals to determine whether they have less virulence and higher immunogenicity before being used to prepare live-attenuated vaccines. Of note, several groups have used cell passage to prepare porcine CoVs attenuated strains, such as PEDV (Lin et al., 2017) and TGEV (Motovski et al., 1985), which laid a good foundation for preparation of live-attenuated vaccines.

PEAV is an important enteropathogen in pigs, but currently no effective treatments or vaccines against PEAV infection are available. To develop a live-attenuated vaccine for PEAV, we generated candidates *via* serial cell passage of the parental PEAV GDS04 strain and evaluated the pathogenicity of PEAV P15, P67 and P100 in 5-day-old newborn piglets. Further, we identified genetic changes related to attenuation by performing comparative, complete genomic sequence analysis of virulent and attenuated PEAV variants.

2. Materials and methods

2.1. Serial virus passaging in Vero cells

Vero cells were obtained from ATCC (ATCC number: CCL-81) (USA), and cultured in Dulbecco' s modified eagle medium (DMEM) (Hyclone, USA) supplemented with 100 U/mL penicillin, 100 U/mL streptomycin, and 10% fetal bovine serum (FBS) (BOVOGEN, Australia). The maintenance medium for PEAV propagation was DMEM supplemented with 10 μg/mL trypsin (Gibco, USA). The isolation and identification of PEAV GDS04 strain were reported previously by our laboratory (Xu et al., 2019a).

Serial virus passaging and plaque-purification in Vero cells were performed as previously described with some modifications (Lin et al., 2017; Xu et al., 2019a). Briefly, Vero cells were cultured in 6-well plates, and washed three times with sterile pH 7.4 1 × phosphate buffer saline (PBS) when 90% confluent. Ten μL of PEAV GDS04 strain together with 2 mL maintenance medium were added to plate and cultured continuously at 37℃ in 5% CO_2 to observe cytopathic effect (CPE). Around 1 day post inoculation (d.p.i.), the plates were frozen at -80℃ and thawed twice after CPE was evident in the inoculated cell monolayers. The cells and supernatants were harvested together and used as seed stocks for the next passage. PEAV GDS04 strain was passaged regularly to a total of 100 passages in Vero cells every 2–3 days and the P15, P67 and P100 were plaque-purified. Finally, T175 flasks were used for the P15, P67 and P100 propagation in Vero cells.

2.2. Pigs

Four-day-old crossbred conventional newborn piglets produced by Duroc × Landrace × Native pigs of Guangdong of China were procured from Wen' s Foodstuffs Group Co, Ltd (Guangdong, China). All pigs were maintained in our animal facility with a mixture of skim milk powder (Inner Mongolia Yi Li Industrial Group Co., Ltd, China) with warm water ad libitum for 1 day before the experimentation. The animal study was approved by the Institutional Animal Care and Use Committee of the Sun Yat-sen University (Guangdong, China) and animals were treated in accordance with the regulations and guidelines of this committee.

2.3. Measurement of virus growth in Vero cells

Kinetics of PEAV replication in Vero cells were performed as previously described with some modifications (Lin et al., 2017). Briefly, Vero cell monolayer was inoculated with P15, P67 and P100 at a MOI = 0.1. The virus inoculum was removed at 2 h post inoculation (hpi), washed with pH 7.4 1 × PBS twice and replaced by the maintenance medium. Culture supernatant and cell lysates were collected at 6, 12, 18, 24 and 30 hpi, respectively. After freezing and thawing once, the mixtures of culture supernatants and cell lysates were subjected to titration for 50% tissue culture infectious dose ($TCID_{50}$) in 96-well plates and calculated using Reed-Muench method (Reed and Muench, 1938).

2.4. Experimental infection of PEAV at selected passages in conventional newborn piglets

Thirty-two 4-day-old conventional newborn piglets were randomly divided into four groups and 8 piglets in each group. Prior to inoculation, piglets were confirmed to be negative for the major porcine enteric viruses including PDCoV, PEDV, TGEV, PRoV, PEAV, by testing of rectal swabs using specific RT-PCR according to previously described method (Xu et al., 2018; Zhou et al., 2018a). In addition, serum of each piglet was collected and a commercial kit (ALLRIGHT BIOTECHONOLOGY, China) was applied in order to detect PEDV-specific antibody according to the manufacturer' instruction. PEDV-specific antibodies were not detected in all sera samples (data not shown). After 1-day acclimation, piglets in group 1 were orally inoculated with 5 mL of maintenance medium and served as uninfected controls. Piglets in group 2, 3 and 4 were orally challenged with 5 mL of maintenance medium containing a total of 5×10^6 $TCID_{50}$ of P15, P67 and P100, respectively. To reduce the risk of cross contamination among piglets and piglet death caused by non-experimental factors, the entire animal study period was ended in nine days after challenge.

All piglets were observed daily for clinical signs of diarrhea and lethargy. Diarrhea severity was scored with the following criteria (Chen et al., 2015): 0 = normal, 1 = soft (cowpie), 2 = liquid with some solid content, 3 = watery with no solid content.

Rectal swabs were collected daily from each piglet from 1 d.p.i. to 9 d.p.i., submerged into 1 mL sterile pH 7.4 1 × PBS immediately after collection and stored at -80℃ for virus shedding analysis. Two piglets from each group were necropsied at 7 d.p.i.. At necropsy, the fresh jejunums were collected and then formalin-fixed. The formalin-fixed samples were used for histopathology and immunohischemistry analysis. In addition, the mortality of newborn piglets in each group was recorded daily.

2.5. RNA isolation and real-time RT-PCR analysis

Viral RNA shedding in piglet feces after infection with PEAV was detected as previously described with some modifications (Xu et al., 2019a). Briefly, total RNA was prepared from the supernatant of rectal swab from each piglet using a RNeasy kit (Magen, China) according to the manufacturer' instruction, and was treated with DNase I. Two μg of total RNA was used for cDNA synthesis by reverse transcription using RT-PCR kit (TaKaRa, Dalian). The specific primers for the *n* gene of PEAV (sense: 5′-CTGACTGTTGTTGAGGTTAC-3′; antisense: 5′-TCTGCC AAAGCTTGTTTAAC-3′), and probe (5′-FAM-TCACAGTCTCGTTCTCGC AATCA-TARMA-3′) were designed with reference to the previous publication (Zhou et al., 2018a) and synthesized by Invitrogen Company (Shanghai, China). The real-time PCR assay was carried out with an Applied Biosystem 7500 instrument (Life Technologies, USA). The PCR was performed in a 20-μL volume containing 1 μL of cDNA, 10 μL of Thunderbird Probe qPCR Mix, 0.04 μL 50 × Rox reference dye (TOYOBO, Shanghai), 0.2 μmol/L of probe, and a 0.3 μmol/L of each gene-specific primer. The thermal cycling parameters were as follows: 95 °C for 30 s; 45 cycles of 95 °C for 5 s, 62 °C for 30 s. And the *n* gene was amplified to generate the standard curve from PEAV GDS04 strain using the specific primers (sense: 5′−CCGCTCGAGATGGCAACTGTTA ATTGG-3′; antisense: 5′-CGCGGATCCCGATTAATAATCTCATCCAC-3′)

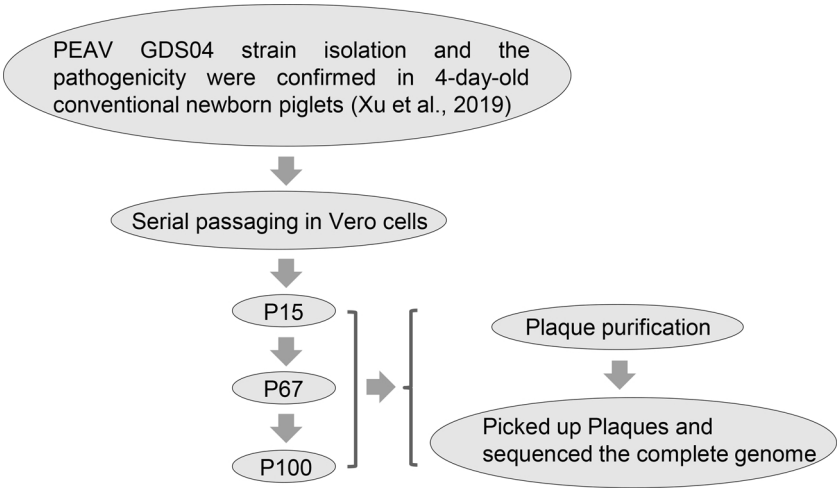

Fig. 1. The flowchart of the isolation and passaging of PEAV GDS04 strain in Vero cells.

that were designed with reference to the published sequence (GenBank, Accession no: MF167434.1), and the PCR products were cloned into the pEGFP-N1 (Clontech, USA). The known plasmid concentration was 10-fold serially diluted for generating a standard curve in each plate. The quantity of PEAV viral RNA in tested samples was calculated based on the cycle threshold (Ct) values for the standard curve.

2.6. Histological and immunohistochemical staining

Histological and Immunohistochemical staining were performed as previously described with some modifications (Xu et al., 2019a). Briefly, tissue samples of jejunum of the piglets from the challenged and control groups were separated, routinely fixed in 10% formalin for 36 h at room temperature, dehydrated in graded ethanol, embedded in paraffin, cut in 5-μm sectioned, and mounted onto glass slides. After the sections were deparaffinized, rehydrated, and stained with hematoxylin and eosin (H&E), the slides were examined and analyzed with conventional light microscopy. Five-μm sections of formalin-fixed paraffin-embedded tissues were placed onto positively charged glass slides and the slides were air dried for 120 min at 60 °C. The tissue sections were deparaffinized, rinsed and incubated with target retrieval solution (Servicebio, China). After being blocked with 1% BSA (Solarbio, China), the sections were incubated with anti-PEAV M monoclonal antibody (Wen's Foodstuffs Group Co., Ltd, China) as the primary antibody and the dilution of antibody was 1:200 for 12 h at 4 °C. They were then incubated with peroxidase-labeled goat anti-mouse IgG secondary antibody (Dako, Denmark) and the dilution of antibody was 1:200 for 50 min at room temperature, and the samples were finally visualized with a 3, 3′-diaminobenzidine (DAB) chromogen kit (Dako, Denmark). Hematoxylin was used for counterstaining. Tissues of piglets from uninfected control groups were used as negative samples. The immunohistochemistry slides were evaluated according to the evaluation system of histology and immunohistochemistry by Jung et al. (2014).

2.7. Genomic sequencing and sequence analysis

The complete genomes of P15, P67 and P100 were sequenced by IlluminaHiSeq as previously described with some modifications (Malboeuf et al., 2013). Briefly, total RNA was prepared from the PEAV-infected Vero cells using a RNeasy kit (Magen, China) according to the manufacturer' instruction, and was purified as described above. cDNA synthesis was performed by reverse transcription using RT-PCR kit (TaKaRa, Dalian). The genomic cDNA was disrupted and converted to a sticky end by adding the A-base at 3′ end of the cDNA. The DNA containing Index sequence was added at either side of sticky end by complementary bases. The target fragment within the scope of a certain length was collected before magnetic beads selection. The sequencing library was built, tested using PCR amplification Index sequence, and combined to the chip by bridge PCR. At last, the complete genome was sequenced by IIIumina HiSeq. A genome homology analysis and phylogenetic trees were constructed by using the maximum likelihood method with MEGA 5 software (http://www.megasoftware.net/) based on the whole-genome nucleotide sequences from PEAV GDS04, P15, P67 and P100 together with other CoVs, like PEDV, PDCoV and TGEV. Sequence alignments of N, M, S and ORF1ab amino acids (aa) of GDS04, P15, P67 and P100 were performed using the DNAMAN.

2.8. Homology modeling of the S proteins of P15, P67 and P100

The S protein of CoV, the pivotal surface glycoprotein, plays an important role in virus attachment and entry, and induction of neutralizing antibodies *in vivo* (Cruz et al., 2008; Li et al., 2017, 2016). To further determine the differences of Vero-passaged PEAV strains, the three-dimensional structures of S proteins of GDS04, P15, P67 and P100 were predicted in SWISS-MODEL using amino acid homology modeling, based on the existing three-dimensional structure of S glycoprotein trimer of Human coronavirus NL63 (PDB code 5SZS) (Walls et al., 2016) in Protein Data Bank. The PyMOL Molecular Graphics System (DeLano Scientific; http://www.pymol.org) was used for figures preparation.

2.9. Statistical analysis

Statistical comparisons were performed using GraphPad Prism software. The significance of the differences between the growth rate of P100 and P15 or P67 in the $TCID_{50}$ was determined by the ANOVA and Mann-Whitney accordingly.

3. Results

3.1. PEAV P100 had highest infectious titers in Vero cells

To generate an attenuated PEAV vaccine candidate, PEAV GDS04 was passaged regularly to a total of 100 passages in Vero cells and the selected passages including P15, P67 and P100 were characterized by sequencing and analyzing the complete genome (Fig. 1). To determine the growth rate of P15, P67 and P100 *in vitro*, we inoculated P15, P67 and P100 at MOI = 0.1 in Vero cells and detected the live virus count at corresponding time point with a $TCID_{50}$ assay. Interestingly, we observed that the sizes of PEAV-induced syncytia increased in P67 and

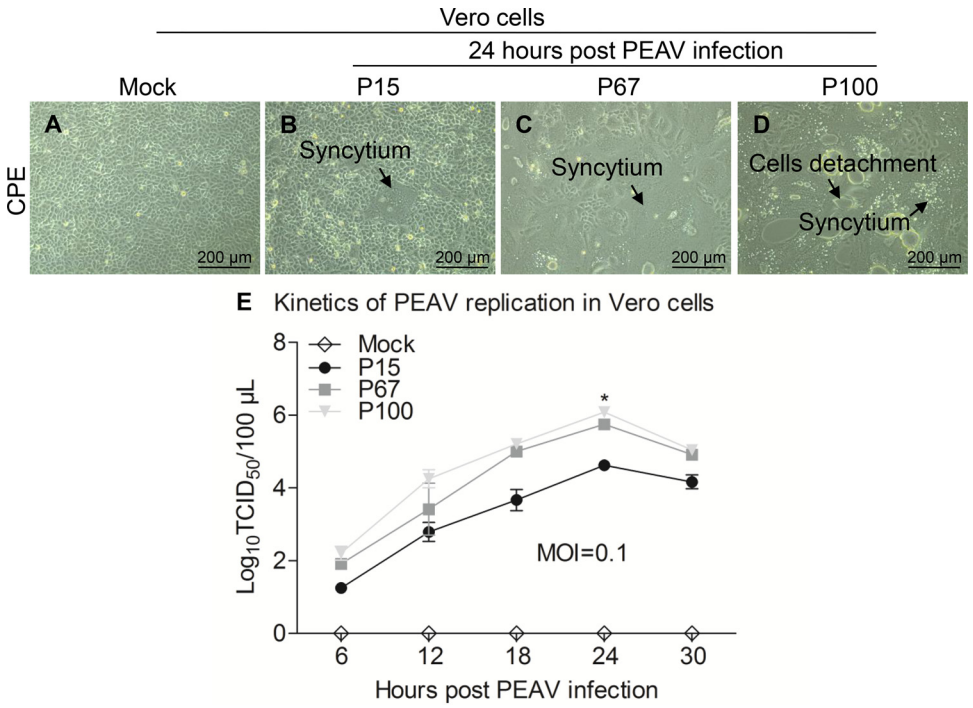

Fig. 2. The growth kinetics of PEAV P15, P67 and P100 in Vero cells.
(A) Mock-inoculated Vero cell culture representing normal cells. (B–D) Vero cells were inoculated with PEAV P15, P67 and P100 at MOI = 0.1. PEAV-inoculated Vero cells at 24 hpi. showing syncytium and cells detachment and was indicated by arrows. (E) Cell lysates were sampled at designated time points and titrated using $TCID_{50}$ infectivity assay. Results are representative of three independent experiments. Data are represented as mean ± SD, n = 3. *stands for $p < 0.05$.

P100 (Fig. 2A). The diameter of P100-syncytia was larger than that of P15 and P67 (Fig. 2A). In addition, the muti-step growth kinetics of PEAV in Vero cells showed similar growth curve trends of P15, P67 and P100, but the titers of P100 were significantly higher than those of P15 and P67 at 24 h.p.i. ($P < 0.05$) (Fig. 2B).

3.2. PEAV P100 demonstrated reduced clinical signs and fecal virus in newborn piglets

To evaluate the pathogenicity of Vero-passaged PEAV strains in newborn piglets, we experimentally infected 5-day-old conventional newborn piglets with P15, P67 and P100 at a dose of 5×10^6 $TCID_{50}$/head *via* oral feeding. As shown in Fig. 3A, the newborn piglets inoculated with P15, P67 or P100 all showed diarrhea from 1 d.p.i. to 9 d.p.i., as compared with the control. But compared to P15 and P67, the degree of diarrhea of the newborn piglets inoculated with P100 was the lowest, indicating that viral pathogenicity decreased gradually in 5-day-old newborn piglets with cell passage. In addition, we explored the fecal viral shedding in PEAV-inoculated piglets from 1 d.p.i. to 9 d.p.i. by qRT-PCR. Consistent with the clinical signs, the amount of virus RNA was lower in P100-inoculated newborn piglets, and no PEAV RNA was detected in the negative control piglets during the study (Fig. 3B). Taken together, these results demonstrated that cell passage gradually decreased viral pathogenicity of GDS04 to 5-day-old newborn piglets.

3.3. PEAV P100 was attenuated in newborn piglets

Since PEAV at selected passages caused varying degrees of diarrhea in newborn piglets, we also recorded the mortality of newborn piglets in each group. As shown in Fig. 4, in P15-inoculated group, except two piglets that were necropsied at 7 d.p.i., 2, 1, 1, and 1 death (s) were recorded at 3, 4, 5, and 8 d.p.i., respectively. Similarly, except two necropsied piglets, 4 piglets in P67-inoculated group died from 5 to 9 d.p.i. No piglets died in P100-inoculated group and the control group except two piglets that were necropsied at 7 d.p.i.. Taken together, these results suggest that PEAV P100 strain is low pathogenic to the newborn piglets.

3.4. PEAV P100 caused reduced lesions and had limited antigen distribution in intestinal tract

To determine the gross pathological and histological changes in piglets infected with PEAV GDS04 at selected passages, two piglets from each group were necropsied at 7 d.p.i. Gross findings were similar in piglets orally inoculated with P15 and P67. The whole intestinal tract, where yellow watery contents accumulated, were transparent, thin-walled, and gas-distended (Fig. 5B&C). No lesions were observed in the whole intestinal tract of the P100-inoculated piglets and the negative control piglets (Fig. 5A&D). Microscopic lesions were also analysed. As shown in Fig. 5F&G, abruption of intestinal villus was observed in P15 or P67-inoculated piglets, whereas the intestines in P100-inoculated piglets and the negative control were normal (Fig. 5E&H). Consistent with the histopathological results, PEAV antigen was detected in the cytoplasm of the villous enterocytes of the P15 or P67-challenged piglets by immunohistochemical analysis, but no antigen observed in P100-inoculated and mock piglets (Fig. 5I-L). Taken together, these results indicate that PEAV P100 is an attenuated variant.

3.5. Phylogenetic analysis of complete-genome and comparison of the aa changes among M, N, S and ORF1ab proteins

To determine the cause of reduced pathogenicity of Vero-passaged PEAV strains, the complete genomes of P15, P67 and P100 were sequenced and analyzed. Compared to the complete genome of PEAV GDS04 (MF167434.1), P15 possesses 3 point mutations, a 3-nt deletion and a 3-nt insertion; P67 possesses 18 point mutations, a 3-nt deletion and a 3-nt insertion; P100 possesses 18 point mutations, a 3-nt deletion, a 6-nt deletion and a 3-nt insertion, respectively (data not shown), presenting a clue of different pathogenicity of these three strains. In addition, the parental strain GDS04 shares 99.97%, 99.91%, 99.89% nucleotide identity with P15, P67 and P100, respectively (data not shown), indicating that differences in viral genome increased gradually with cell passages. In spite of some differences in viral genome of these strains, phylogenetic analysis showed that PEAV GDS04, P15, P67 and P100 were clustered into a large clade (Fig. 6A). We further analyzed the aa of proteins which might be associated with the pathogenicity of CoVs, such as M (Zhang et al., 2016), N (Hu et al., 2017) and S proteins

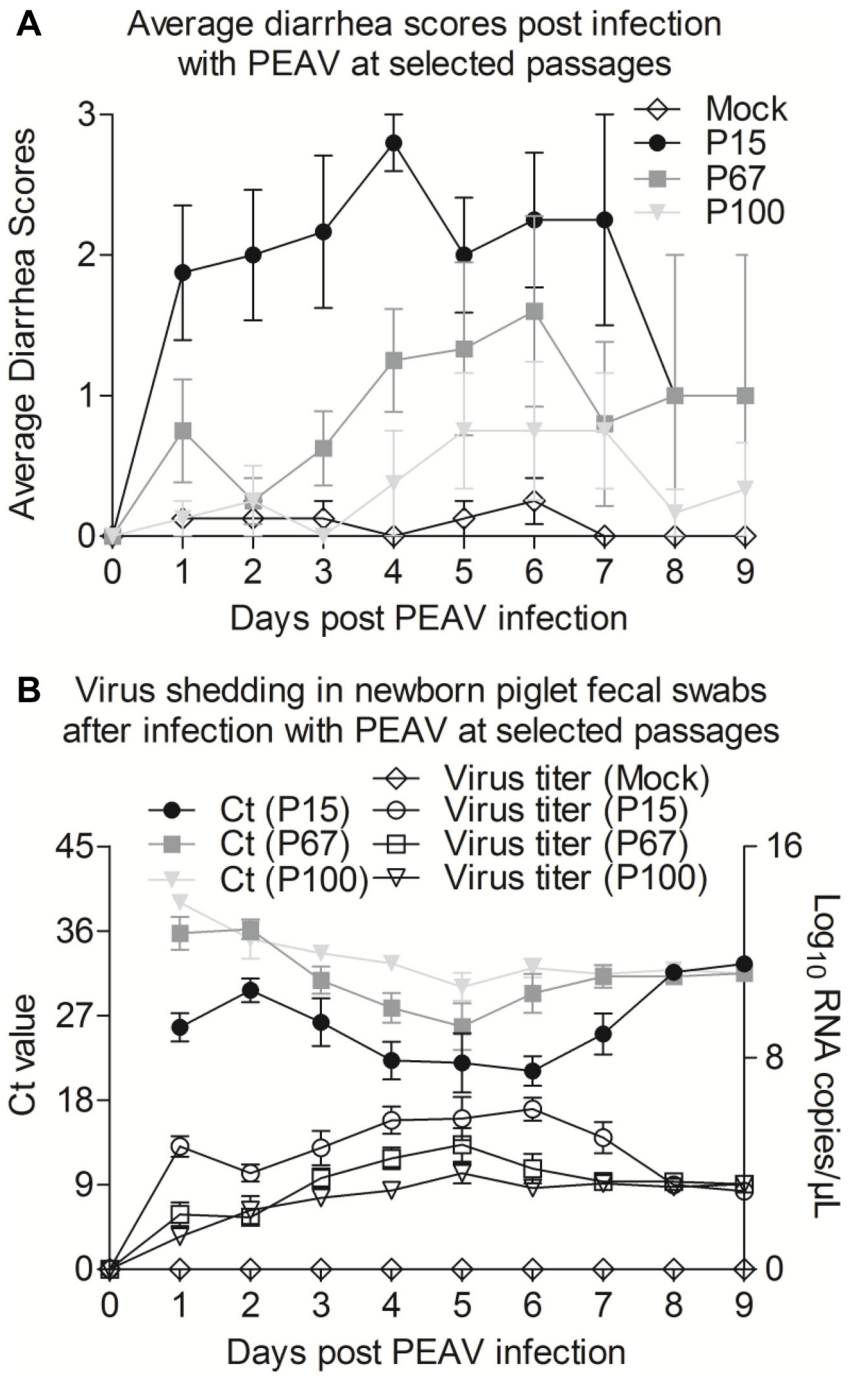

Fig. 3. Clinical signs and fecal viral shedding in newborn piglets inoculated with PEAV P15, P67 and P100 *via* oral feeding.
(A) Average diarrhea scores after P15, P67 and P100 infection. (B) Ct values and copies of PEAV RNA of feces from piglets after P15, P67 and P100 or mock inoculation.

(Hou et al., 2019b). As shown in Fig. 6B, compared to the M protein of PEAV GDS04, P15 possesses 2 aa mutations, P67 possesses 3 aa mutations, and P100 possesses 4 aa mutations. Compared to the N protein of PEAV GDS04, interestingly, only P100 possesses 1 aa mutation, while no mutations were observed in P15 and P67. Compared to the S protein of PEAV GDS04, P15 possesses 1 aa mutation, P67 possesses 3 aa mutations, while P100 possesses 3 aa mutations and 3 aa deletions. In addition, compared to the ORF1ab protein of PEAV GDS04, P15 possesses 2 aa mutations, 2 aa insertions, P67 possesses 10 aa mutations, 2 aa insertions, P100 possesses 8 aa mutations, 1 aa deletion and 2 aa insertions. The detailed information of aa changes might help to explain the low pathogenicity of P100 to the newborn piglets.

3.6. PEAV P100 has significant differences in the S protein structure

Considering the obvious aa mutations and deletions in S proteins of Vero-passaged PEAV strains, we attempted to predict and analyze the three-dimensional structures of S proteins of these PEAV strains. After analysing the amino acid sequences, the S protein in GDS04 was found to have 27.68% identity with the S protein of Human CoV NL63 (Walls et al., 2016) The S protein structures of these strains were predicted by SWISS-MODEL, using the S protein of Human CoV NL63 as the template (Fig. 7). The predicted structure of GDS04 S protein forms a homologous trimer with an expect-value of 0.36, and each monomer is composed of 983 residues in the aa positions 31–1013 (Fig. 7A&B). In

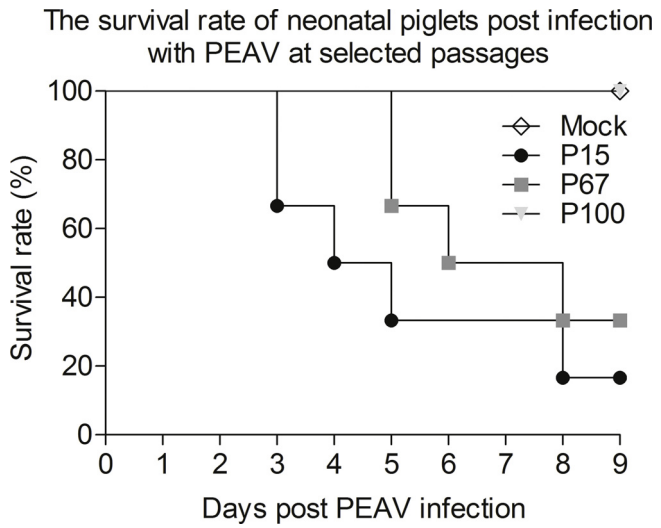

Fig. 4. The survival rate of newborn piglets after infection with PEAV P15, P67 and P100.
The mortality of newborn piglets in each group was recorded from 1 to 9 d.p.i..

addition, the predicted three-dimensional structures of the S proteins of PEAV P15, P67 and P100 have similar overall structures when compared with GDS04 S protein (Fig. 7C-F). However the monomer structural overlap of the four S proteins showed that there were three loops and two β strands having significant structural differences in the main chain, especially between P100 and GDS04.

4. Discussion

Since the first report of PEAV in pigs in early February of 2017 in Guangdong, China (Gong et al., 2017), this novel swine enteric CoV has been widely detected in Guangdong, China, with a prevalence of 43.53% and an emergence in China as early as August 2016 by a retrospective detection study (Zhou et al., 2019). Although a few studies have demonstrated PEAV was highly pathogenic to newborn piglets (Pan et al., 2017; Xu et al., 2019a; Zhou et al., 2018b), there are no effective treatments or any vaccines against PEAV infection. In the present study, attenuated PEAV variants were generated by serial cell passaging and orally inoculated to newborn piglets to evaluate the attenuation *in vivo*. Further, we identified the molecular basis of attenuation by performing comparative, complete genomic sequence analysis of virulent and attenuated PEAV variants.

Swine enteropathogenic CoVs affects all sectors of the pig industry and all cycles of production, which results in significant economic losses. Currently, vaccination remains the most effective measure against swine enteropathogenic CoVs. Of note, several groups have used live-attenuated vaccines to prevent and control PEDV and TGEV in pigs (Aynaud et al., 1991; Song et al., 2007). As a newly swine enteropathogenic CoV, there are no reports about live-attenuated vaccine for PEAV. Pathogenic microorganisms serially passaged in cells (Jie et al., 2018) is one of the most common methods to prepare live-attenuated vaccine. Vero cells as a stable African green monkey kidney cell line (Rhim et al., 1969) is commonly used to attenuate CoVs like PEDV (Lin et al., 2017). In this study, PEAV GDS04 was passaged regularly to a total of 100 passages in Vero cells and the growth rate of P15, P67 and P100 was determined *in vitro*. The muti-step growth kinetics of P15, P67 and P100 in Vero cells were similar, but the titers of P100 were

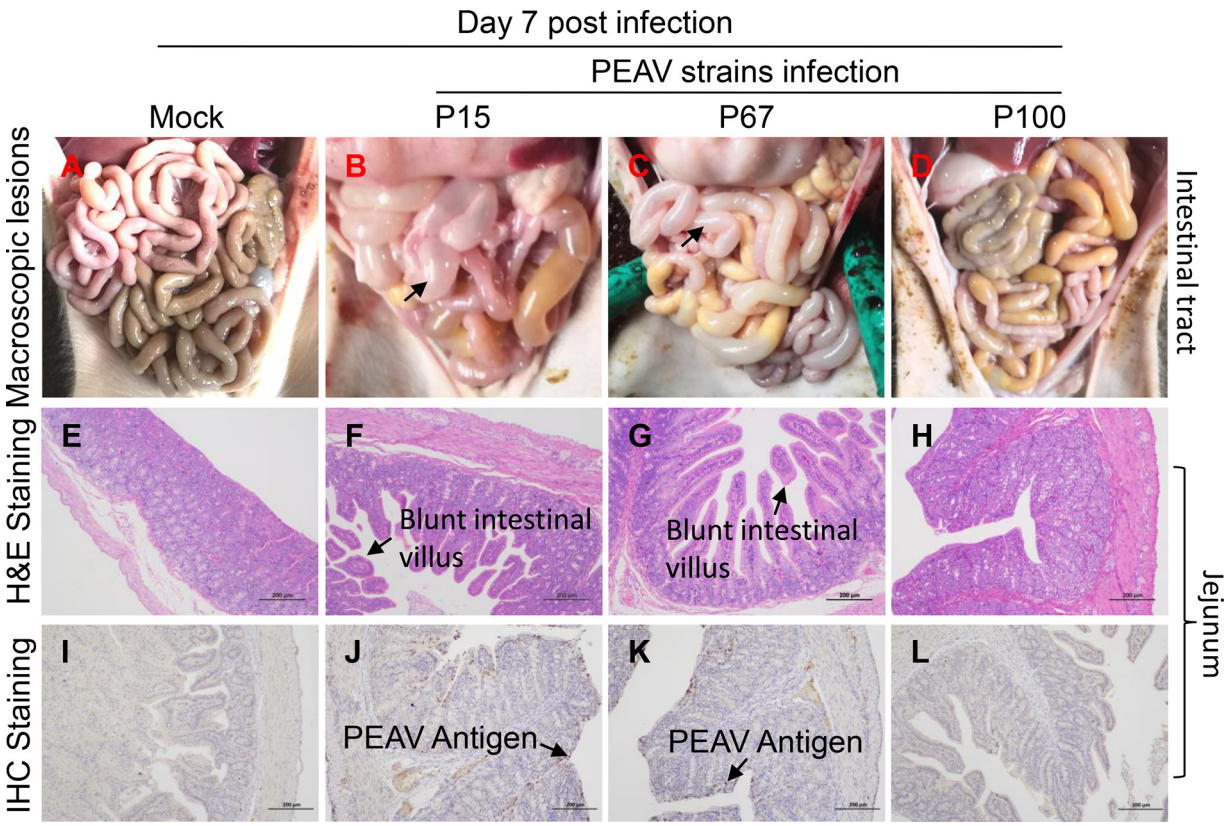

Fig. 5. Intestinal changes in newborn piglets inoculated with PEAV P15, P67 and P100.
(A) Macroscopic picture of intestine from a control piglet at 7 d.p.i. (B–D) Macroscopic pictures of intestine from P15, P67 and P100-challenged newborn piglets at 7 d.p.i. Thin-walled intestinal tracts were indicated by arrows. (E) H&E-stained jejunum tissue section of a control piglet at 7 d.p.i. (F-H) H&E-stained jejunum tissue section of P15, P67 and P100-challenged piglet at 7 d.p.i. Blunt intestinal villus was indicated by arrows. (I) Immunohistochemically stained jejunum tissue section of a control piglet at 7 d.p.i. (J–L) Immunohistochemically stained jejunum tissue section of P15, P67 and P100-challenged piglet at 7 d.p.i..

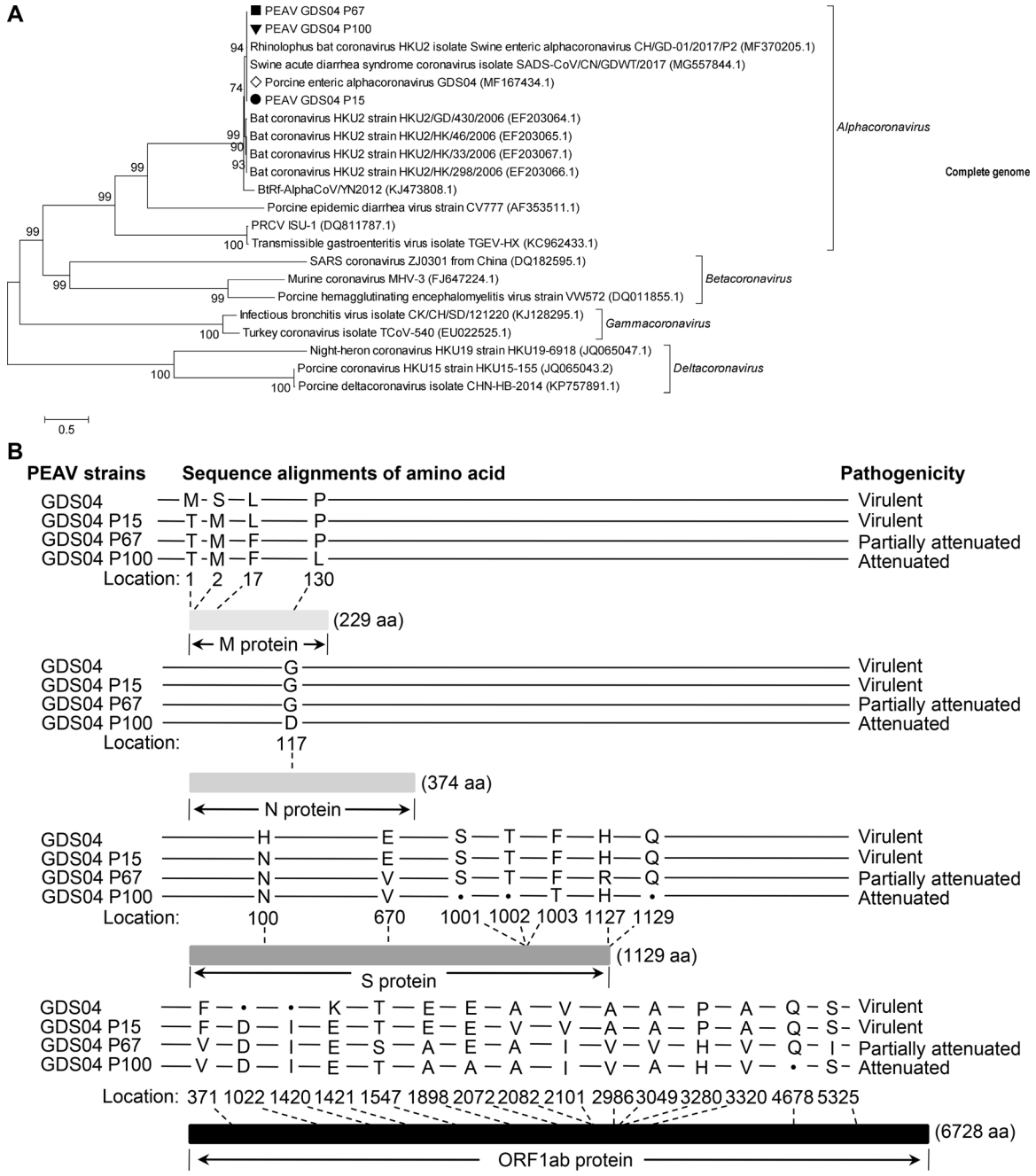

Fig. 6. Phylogenetic trees constructed on the basis of the complete genome sequences of PEAV P15, P67 and P100 or other CoVs and sequence alignments of PEAV at selected passages.

(A) The dendrogram was constructed using the neighbour-joining method in the MEGA software package, version 5 (http://www.megasof tware.net). Bootstrap resampling with 1,000 replicates was performed, and bootstrap values are indicated for each node. Reference sequence obtained from GenBank is indicated by strain name. The scale bar represents 0.5 nucleotide substitutions per site. (B) Sequence alignments of the amino acids of M, N S and ORF1ab proteins were performed using DNAMAN software.

significantly higher than those of P15 and P67 at 24 hpi, similar to observations in attenuated PEDV vaccine (Lin et al., 2017), indicating that P100 had better adaptation in cells *in vitro*. Usually, adaptation in cell lines coincides with attenuation of the viruses, such as African swine fever virus (ASFV) isolate Georgioa and PEDV isolate PC22A, in swine (Krug et al., 2015; Lin et al., 2017). The higher fitness of P100 in Vero cells might suggest the changed pathogenicity of PEAV.

For a vaccine candidate, safety is the top concern. It was reported that swine enteric CoVs like PDCoV, PEDV and TGEV are age-dependent disease (Moon et al., 1975; Shibata et al., 2000; Xu et al., 2019b). Similarly, in another study, we found that PEAV was highly pathogenic to newborn piglets (Xu et al., 2019a), but did not cause vomiting and death in weaned piglets at a medium dose of 1×10^6 $TCID_{50}$ within 7 days (data not shown), for which reason we choose newborn piglets to conduct PEAV pathogenicity study. It was known that PEAV infection caused typical clinical symptoms characterized by watery diarrhea *via* oral feeding in newborn piglets (Xu et al., 2019a). In the study, we infected the 5-day-old newborn piglets with P15, P67 and P100 *via* oral feeding. Compared with P15 and P67, P100 caused slight diarrhea in newborn piglets, suggesting that the pathogenicity of PEAV changed through cell passage. For enteric viruses, viral shedding is often accompanied by diarrhea, so was PEAV infection (Xu et al., 2019a). Thus,

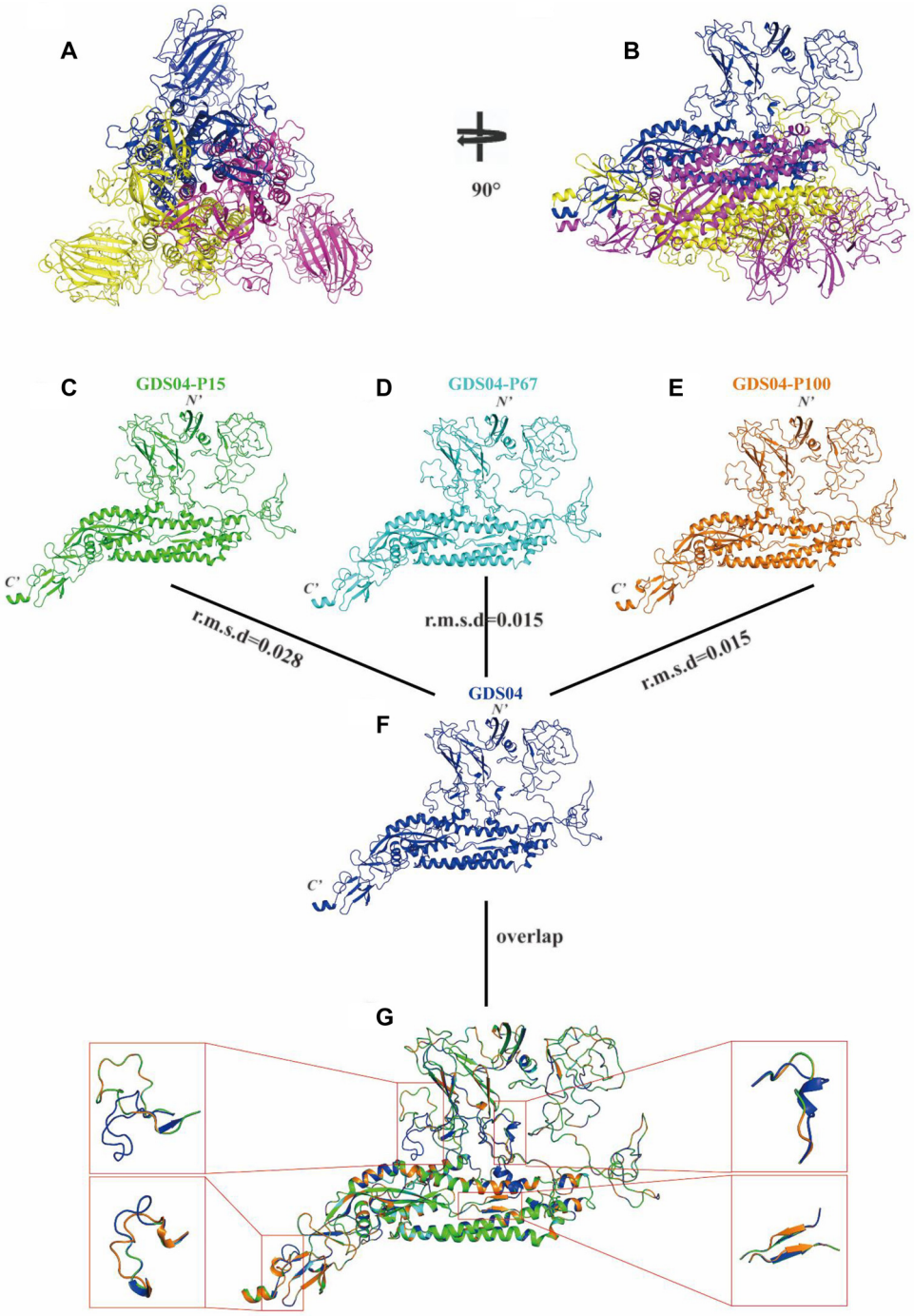

Fig. 7. Structural analysis of the S proteins of PEAV GDS04, P15, P67 and P100.
All the predicted structures of S protein were shown in cartoon style with different colors. Blue, yellow and purple stand for GDS04; green stands for P15; cyan stands for P67; orange stands for P100. (A&B) The predicted overall structure of S protein of PEAV GDS04 strain. (C–F) Three-dimensional structure of the monomer S protein in P15 (C), P67 (D), P100 (E) and GDS04 strain (F). (G) Structural overlap of the S proteins of PEAV at selected passages.

we collected fecal swabs from the PEAV-challenged piglets and detected the fecal shedding by real-time PCR. Consistent with the clinical signs, the amount of virus RNA was lower in P100-inoculated newborn piglets. Interestingly and importantly, the presence of PEAV RNA in fecal samples of P100 inoculated piglets from 1 d.p.i to 9 d.p.i suggested the successful colonization and replication of P100 in intestinal tract, which is essential to induce mucosal immunity for an enteric pathogen vaccine candidate. It was reported that the lesions were only observed in intestinal tract but not any other organs after PEAV infection and PEAV antigen was detected in the villous enterocytes of the PEAV-challenged piglets (Xu et al., 2019a). Compared to P15 and P67, P100 strain caused slight macroscopic and microscopic lesions in intestinal tract and no PEAV antigen was detected in the cytoplasm of the villous enterocytes of the P100-challenged newborn piglets by immunohistochemical analysis, indicating that the infectiveness of P100 was reduced. Like other swine enteric CoVs, such as PEDV (Shibata et al., 2000), PEAV infection caused fatal disease in newborn piglets (Xu et al., 2019a). Thus, death after infection is the key indicator to determine the attenuation of the viral strain. Compared to P15 and P67, no piglets died in P100-inoculated group and the control group during the study,

indicating that P100 is low pathogenic to the newborn piglets. Taken together, these results demonstrated that P100 strain is safe for pigs and effective in colonizing and replicating in intestine, suggesting its future application as a good PEAV vaccine candidate.

Compared to P15 and P67 strains, the virulence of P100 was significantly reduced in 5-day-old newborn piglets. The S protein of CoVs is the pivotal surface glycoprotein involved in virus attachment and entry, virus attenuation and induction of neutralizing antibodies *in vivo* (Cruz et al., 2008; Lin et al., 2017; Woo et al., 2010). In addition, the virulence of a recombinant PEDV with inactivation of the endocytosis signal of the S protein was significantly reduced in piglets (Hou et al., 2019a), indicating that the S protein might be associated with the virulence of CoVs. Compared to the S protein of parental strain GDS04, P100 possesses 2 aa mutations in aa positions 100 and 670, which were also found in P15 and P67, indicating that these 2 aa-mutations are insufficient to cause viral attenuation. Of note, Compared to P15 and P67, P100 possesses 3 aa deletions and 1 aa mutation in aa positions 1001, 1002, 1003 and 1129, respectively, indicating that the absence and mutation of these amino acids might affect the viral attenuation. Usually, protein with complete structure has corresponding function, and the changes in the protein's structure might affect its function. Overlap of the S protein structures of GDS04, P15, P67 and P100 showed that the difference between P100 and GDS04 was most significant (Fig. 7), indicating a potential relationship between these differences of S protein and pathogenicity of PEAV. It was reported that the S protein is necessary but not sufficient for the virulence of PEDV (Wang et al., 2018). M protein plays an important role in the process of virus assembly by interacting with S and N proteins (de Haan et al., 1999; Nguyen and Hogue, 1997). N protein can encapsulate the viral genome RNA to form the nucleocapsid (Spaan et al., 1983; Sturman et al., 1980). Inactivation of the viral 2′-O methyltransferase of nsp16 could help to engineer a live attenuated PEDV vaccine (Hou et al., 2019a). In this study, aa changes were also found in M, N and ORF1ab proteins in P100 strain as compared to GDS04 (Fig. 6B). In addition, no additional mutation was observed by sequencing the viruses shed from the challenged piglets (data not shown). Therefore, these results suggest that the complete attenuation of a PEAV strain might be the result of a combination of multiple mutations along the genome, and can occur *via* multiple molecular mechanisms. Whether individual or a combination of genetic changes of PEAV strains alter viral infectivity, pathogenicity and replication efficiency need further examination by reverse genetics technology. Together, all these results confirmed that P100 generated in this study was low pathogenic to the newborn piglets and might serve as a good PEAV vaccine candidate. However, there are still several important questions needed to be addressed. For instance, what is the immunogenicity of P100 strain as a live-attenuated vaccine candidate in pigs? What is the protective effect of P100 strain in pigs? Elucidation of these questions will help us to develop a safe and efficacious live-attenuated vaccine to control PEAV.

In summary, our research successfully generated an attenuated PEAV variant P100. P100 has the highest titers of virus load, *via* serial passaging of the parental GDS04 strain. Remarkably, inoculation of newborn piglets with P100 by oral feeding caused the lowest level of clinical symptoms, including slight diarrhea, fecal viral shedding, and pathological changes with a survival rate of 100% in newborn piglets. The changes in genomic composition and structures found in P100 by genomic analysis might account for the underlying molecular mechanisms of PEAV attenuation.

Author contributions

CYX, ZCX and YL conceived and designed the experiments; ZCX, YL, PP, YW, YL performed the experiments; ZCX analyzed the data; YCC, CYX, CCZ and LG contributed reagents/materials/analysis tools; ZCX wrote the paper. CYX checked and finalized the manuscript. All authors read and approved the final manuscript.

Ethical approval

The animal study was supervised by the Institutional Animal Care and Use Committee of Sun Yat-sen University (IACUC DD-17-1003) and used in accordance with regulation and guidelines of this committee.

Declaration of Competing Interest

The authors declare that they have no conflict interest.

Acknowledgements

This work was supported by National Key Research and Development Program, China (2018YFD0501102), Guangdong Natural Science Foundation (2018B030314003) and the Fundamental Research Funds for the Central Universities (19lgpy188).

References

Aynaud, J.M., B.S, Bottreau, E., Lantier, I., Salmon, H., Vannier, P., 1991. Induction of lactogenic immunity to transmissible gastroenteritis virus of swine using an attenuated coronavirus mutant able to survive in the physicochemical environment of the digestive tract. Vet. Microbiol. 26, 227–239.

Blanco-Lobo, P., Nogales, A., Rodriguez, L., Martinez-Sobrido, L., 2019. Novel approaches for the development of live attenuated influenza vaccines. Viruses 11.

Chen, Q., Gauger, P., Stafne, M., Thomas, J., Arruda, P., Burrough, E., Madson, D., Brodie, J., Magstadt, D., Derscheid, R., Welch, M., Zhang, J., 2015. Pathogenicity and pathogenesis of a United States porcine deltacoronavirus cell culture isolate in 5-day-old neonatal piglets. Virology 482, 51–59.

Cruz, D.J., Kim, C.J., Shin, H.J., 2008. The GPRLQPY motif located at the carboxy-terminal of the spike protein induces antibodies that neutralize Porcine epidemic diarrhea virus. Virus Res. 132, 192–196.

de Haan, C.A., S.M, Vernooij, F., Vennema, H., Rottier, P.J., 1999. Mapping of the coronavirus membrane protein domains involved in interaction with the spike protein. J. Virol. 73, 7441–7452.

Gong, L., L.J, Zhou, Q., Xu, Z., Chen, L., Zhang, Y., Xue, C., Wen, Z., Cao, Y., 2017. A new Bat-HKU2-like coronavirus in Swine, China, 2017. Emerg. Infect. Dis. 23.

Hou, Y., Ke, H., Kim, J., Yoo, D., Su, Y., Boley, P., Chepngeno, J., Vlasova, A.N., Saif, L.J., Wang, Q., 2019a. Engineering a live attenuated PEDV vaccine candidate via inactivation of the viral 2′-O methyltransferase and the endocytosis signal of the spike protein. J. Virol.

Hou, Y., Meulia, T., Gao, X., Saif, L.J., Wang, Q., 2019b. Deletion of both the tyrosine-based endocytosis signal and the endoplasmic reticulum retrieval signal in the cytoplasmic tail of spike protein attenuates porcine epidemic diarrhea virus in pigs. J. Virol. 93.

Hu, Y., L.W, Gao, T., Cui, Y., Jin, Y., Li, P., Ma, Q., Liu, X., Cao, C., 2017. The severe acute respiratory syndrome coronavirus nucleocapsid inhibits type I interferon production by interfering with TRIM25-Mediated RIG-I ubiquitination. J. Virol. 91.

Jie, T., Benqiang, L., Jinghua, C., Ying, S., Huili, L., 2018. Preparation and characterization of an attenuated porcine epidemic diarrhea virus strain by serial passaging. Arch. Virol. 163, 2997–3004.

Jung, K., Wang, Q., Scheuer, K.A., Lu, Z., Zhang, Y., Saif, L.J., 2014. Pathology of US porcine epidemic diarrhea virus strain PC21A in gnotobiotic pigs. Emerg. Infect. Dis. 20, 662–665.

Krug, P.W., Holinka, L.G., O'Donnell, V., Reese, B., Sanford, B., Fernandez-Sainz, I., Gladue, D.P., Arzt, J., Rodriguez, L., Risatti, G.R., Borca, M.V., 2015. The progressive adaptation of a georgian isolate of African swine fever virus to vero cells leads to a gradual attenuation of virulence in swine corresponding to major modifications of the viral genome. J. Virol. 89, 2324–2332.

Lau, S.K., Woo, P.C., Li, K.S., Huang, Y., Wang, M., Lam, C.S., Xu, H., Guo, R., Chan, K.H., Zheng, B.J., Yuen, K.Y., 2007. Complete genome sequence of bat coronavirus HKU2 from Chinese horseshoe bats revealed a much smaller spike gene with a different evolutionary lineage from the rest of the genome. Virology 367, 428–439.

Li, C., Li, W., Lucio de Esesarte, E., Guo, H., van den Elzen, P., Aarts, E., van den Born, E., Rottier, P.J.M., Bosch, B.J., 2017. Cell attachment domains of the porcine epidemic diarrhea virus spike protein are key targets of neutralizing antibodies. J. Virol. 91.

Li, K., Bi, Z., Gu, J., Gong, W., Luo, S., Zhang, F., Song, D., Ye, Y., Tang, Y., 2018. Complete genome sequence of a novel swine acute diarrhea syndrome coronavirus, CH/FJWT/2018, isolated in Fujian, China, in 2018. Microbiol. Resour. Announc. 7.

Li, W., van Kuppeveld, F.J.M., He, Q., Rottier, P.J.M., Bosch, B.J., 2016. Cellular entry of the porcine epidemic diarrhea virus. Virus Res. 226, 117–127.

Lin, C.M., Hou, Y., Marthaler, D.G., Gao, X., Liu, X., Zheng, L., Saif, L.J., Wang, Q., 2017. Attenuation of an original US porcine epidemic diarrhea virus strain PC22A via serial cell culture passage. Vet. Microbiol. 201, 62–71.

Malboeuf, C.M., Yang, X., Charlebois, P., Qu, J., Berlin, A.M., Casali, M., Pesko, K.N., Boutwell, C.L., DeVincenzo, J.P., Ebel, G.D., Allen, T.M., Zody, M.C., Henn, M.R., Levin, J.Z., 2013. Complete viral RNA genome sequencing of ultra-low copy samples by sequence-independent amplification. Nucleic Acids Res. 41, e13.

Moon, H.W., K.L, Lambert, G., Stark, S.L., Booth, G.D., 1975. Age-dependent resistance to transmissible gastroenteritis of swine. III. Effects of epithelial cell kinetics on

coronavirus production and on atrophy of intestinal villi. Vet. Pathol. 12, 434–445.
Motovski, A., Katevska, V., Belopopska, P., Naïdenova, N., Veleva, E., 1985. Experiments to produce an attenuated strain of the transmissible gastroenteritis virus and its use as a live vaccine. Vet. Med. Nauki. 22, 3.
Nguyen, V.P., Hogue, B.G., 1997. Protein interactions during coronavirus assembly. J. Virol. 71, 9278–9284.
O'Donnell, V., Holinka, L.G., Gladue, D.P., Sanford, B., Krug, P.W., Lu, X., Arzt, J., Reese, B., Carrillo, C., Risatti, G.R., Borca, M.V., 2015. African swine fever virus georgia isolate harboring deletions of MGF360 and MGF505 genes is attenuated in swine and confers protection against challenge with virulent parental virus. J. Virol. 89, 6048–6056.
Pan, Y., Tian, X., Qin, P., Wang, B., Zhao, P., Yang, Y.L., Wang, L., Wang, D., Song, Y., Zhang, X., Huang, Y.W., 2017. Discovery of a novel swine enteric alphacoronavirus (SeACoV) in southern China. Vet. Microbiol. 211, 15–21.
Reed, L.J., Muench, H., 1938. A simple method of estimating fifty per cent endpoints. Am. J. Epidemiol. 27.
Rhim, J.S., S.K, Creasy, B., Case, W., 1969. Biological characteristics and viral susceptibility of an African green monkey kidney cell line (Vero). Proc. Soc. Exp. Biol. Med. 132, 670–678.
Shibata, I., T.T, Mori, M., Ono, M., Sueyoshi, M., Uruno, K., 2000. Isolation of porcine epidemic diarrhea virus in porcine cell cultures and experimental infection of pigs of different ages. Vet. Microbiol. 72, 173–182.
Song, D.S., Oh, J.S., Kang, B.K., Yang, J.S., Moon, H.J., Yoo, H.S., Jang, Y.S., Park, B.K., 2007. Oral efficacy of Vero cell attenuated porcine epidemic diarrhea virus DR13 strain. Res. Vet. Sci. 82, 134–140.
Spaan, W., D.H, Skinner, M., Armstrong, J., Rottier, P., Smeekens, S., van der Zeijst, B.A., Siddell, S.G., 1983. Coronavirus mRNA synthesis involves fusion of non-contiguous sequences. EMBO J. 2, 1839–1844.
Sturman, L.S., H.K, Behnke, J., 1980. Isolation of coronavirus envelope glycoproteins and interaction with the viral nucleocapsid. J. Virol. 33, 449–462.
Walls, A.C., Tortorici, M.A., Frenz, B., Snijder, J., Li, W., Rey, F.A., DiMaio, F., Bosch, B.J., Veesler, D., 2016. Glycan shield and epitope masking of a coronavirus spike protein observed by cryo-electron microscopy. Nat. Struct. Mol. Biol. 23, 899–905.
Wang, D., Ge, X., Chen, D., Li, J., Cai, Y., Deng, J., Zhou, L., Guo, X., Han, J., Yang, H., 2018. The S gene is necessary but not sufficient for the virulence of porcine epidemic diarrhea virus novel variant strain BJ2011C. J. Virol. 92.
Woo, P.C., Huang, Y., Lau, S.K., Yuen, K.Y., 2010. Coronavirus genomics and bioinformatics analysis. Viruses 2, 1804–1820.
Xu, Z., Zhang, Y., Gong, L., Huang, L., Lin, Y., Qin, J., Du, Y., Zhou, Q., Xue, C., Cao, Y., 2019a. Isolation and characterization of a highly pathogenic strain of Porcine enteric alphacoronavirus causing watery diarrhoea and high mortality in newborn piglets. Transbound. Emerg. Dis. 66, 119–130.
Xu, Z., Zhong, H., Huang, S., Zhou, Q., Du, Y., Chen, L., Xue, C., Cao, Y., 2019b. Porcine deltacoronavirus induces TLR3, IL-12, IFN-alpha, IFN-beta and PKR mRNA expression in infected Peyer's patches in vivo. Vet. Microbiol. 228, 226–233.
Xu, Z., Zhong, H., Zhou, Q., Du, Y., Chen, L., Zhang, Y., Xue, C., Cao, Y., 2018. A highly pathogenic strain of porcine deltacoronavirus caused watery diarrhea in newborn piglets. Virol. Sin. 33, 131–141.
Zhang, Q., Shi, K., Yoo, D., 2016. Suppression of type I interferon production by porcine epidemic diarrhea virus and degradation of CREB-binding protein by nsp1. Virology 489, 252–268.
Zhou, L., Sun, Y., Lan, T., Wu, R., Chen, J., Wu, Z., Xie, Q., Zhang, X., Ma, J., 2019. Retrospective detection and phylogenetic analysis of swine acute diarrhoea syndrome coronavirus in pigs in southern China. Transbound. Emerg. Dis. 66, 687–695.
Zhou, L., Sun, Y., Wu, J.L., Mai, K.J., Chen, G.H., Wu, Z.X., Bai, Y., Li, D., Zhou, Z.H., Cheng, J., Wu, R.T., Zhang, X.B., Ma, J.Y., 2018a. Development of a TaqMan-based real-time RT-PCR assay for the detection of SADS-CoV associated with severe diarrhea disease in pigs. J. Virol. Methods 255, 66–70.
Zhou, P., Fan, H., Lan, T., Yang, X.L., Shi, W.F., Zhang, W., Zhu, Y., Zhang, Y.W., Xie, Q.M., Mani, S., Zheng, X.S., Li, B., Li, J.M., Guo, H., Pei, G.Q., An, X.P., Chen, J.W., Zhou, L., Mai, K.J., Wu, Z.X., Li, D., Anderson, D.E., Zhang, L.B., Li, S.Y., Mi, Z.Q., He, T.T., Cong, F., Guo, P.J., Huang, R., Luo, Y., Liu, X.L., Chen, J., Huang, Y., Sun, Q., Zhang, X.L., Wang, Y.Y., Xing, S.Z., Chen, Y.S., Sun, Y., Li, J., Daszak, P., Wang, L.F., Shi, Z.L., Tong, Y.G., Ma, J.Y., 2018b. Fatal swine acute diarrhoea syndrome caused by an HKU2-related coronavirus of bat origin. Nature 556, 255–258.